Revista de la Sociedad Geológica de España 30 (1)

ISSN (versión impresa): 0214-2708
ISSN (Internet): 2255-1379

SEDIMENTARY ANALYSIS OF *MUD PATCH* FIELDS IN THE SUBTIDAL ZONE OF THE CÁDIZ BAY (SW SPAIN)

Análisis sedimentario de los campos de parches de fango presentes en la zona submareal de la Bahía de Cádiz (SO de España)

José Manuel Gutiérrez Mas[1], Coral Cepeda Jorge[1] and Oscar Alvarez Esteban[2]

[1] *Department of Earth Sciences (Cadiz University). Polígono Río San Pedro, 11510-Puerto Real (Cádiz, Spain). josemanuel.gutierrez@uca.es; coral.cepeda@gmail.com*
[2] *Department of Physical Oceanography (Cádiz University. Polígono Río San Pedro, 11510-Puerto Real (Cádiz, Spain). oscar.alvarez@uca.es*

Abstract: *In the subtidal zone close to the northern edge from the Cádiz Bay (SW Spain), between the Rota harbour and the La Galera shoal, several mud patch fields have been identified through side scan sonar records. These appear in the sonographic records as patches of whitish colour, which are surrounded by dark-grey sands. In order to establish the factors that control the presence of these bedform fields, a sedimentological study has been carried out. The results indicate that the normal hydrodynamic agents, such as tidal currents and waves, did not have capacity to cause these morphologies, therefore, other factors are necessary to explain their formation. Depositional processes, such as, hydrated gas scape, major storms, earthquakes and tsunamis, could cause the reactivation and reworking of these bedforms, but they did not cause their formation. The data indicate that the underwater landslides are related to the presence of submarine outcrops of Miocene diatomite marls, which constitute the continuity seaward of diatomite marls that outcrop in the coastal cliff from the nearby Almirante beach. Both emerged and submerged outcrops show numerous lobed morphologies caused by surface erosion and gravitational slides, which must have been formed in terrestrial environments, before the sea reached its current level. Later, the submerged outcrops were modified by the tides and waves, as well as by the action of other processes and events that partially modified the deposits.*

Key-words: *Cádiz Bay, submarine landslides, mud patches, diatomite marls.*

Resumen: *En la zona submareal cercana al margen norte de la Bahía de Cádiz (SO España), entre el puerto de Rota y el bajo de La Galera, se han identificado varios campos de parches de fango, que han sido cartografiados mediante sonar de barrido lateral. Estos aparecen en los registros como manchas de color blanquecino, rodeados de arena de color gris oscuro. Con objeto de establecer los factores que controlan la existencia de estas morfologías, se ha realizado un estudio sedimentológico de la zona, cuyos resultados han permitido caracterizar la morfología y origen de los deslizamientos y los factores que controlan su permanencia en el fondo. Los resultados indican que los deslizamientos submarinos están relacionados con la existencia de afloramientos sumergidos de margas diatomíferas de edad Mioceno superior, que representan la continuación mar adentro de materiales de la misma naturaleza que afloran en el acantilado de la cercana playa del Almirante. Tanto los afloramientos margosos emergidos como los sumergidos, muestran abundantes morfologías lobuladas relacionadas con procesos de erosión superficial y deslizamientos gravitatorios que tuvieron lugar en ambientes subaéreos, antes de que el mar alcanzase su nivel actual. Más tarde, la parte sumergida del afloramiento fue modificada por las mareas y el oleaje, así como por la acción de otros procesos y eventos que modificaron parcialmente los depósitos.*

Palabras clave: *Bahía de Cádiz, deslizamientos submarinos, parches de fango, margas diatomíferas.*

Gutiérrez Mas, J.M., Cepeda Jorge, C. and Alvarez Esteban, O. (2017): Sedimentary analysis of *mud patch* fields in the subtidal zone of the Cádiz Bay (SW Spain). *Revista de la Sociedad Geológica de España,* 30(1): 41-54.

The studies on submarine landslides in shallow sea bottoms from the Gulf of Cádiz are scarce, maybe because these morphologies are uncommon or have not yet been detected. However, this is not so in the case of deeper waters, such as the external continental shelf and slope, where recent studies show the presence of landslides on the bottom (Pajarón *et al.*, 2015; Vazquez *et al.*, 2015).

Regarding the Cádiz Bay, from the 2000 AD, the existence of *mud patch* fields is known in subtidal environments close to the northern coast, between Rota, Santa Catalina Point and La Galera shoal (Lobo *et al.*, 2000; Parrado Román *et al.*, 2000a, b; Gutiérrez Mas *et al.*, 2009b). According to the model of Coleman and Prior (1981), Parrado Román *et al.* (2000a, b) interpreted these morphologies as submarine landslides, those origin was attributed to the marine agent action on a muddy-sandy bottom. However, the critical review of the older data, together with results obtained from the new sedimentological investigations performed in the present work, indicate that these *mud patch* fields are not only a consequence of the action of the hydrodynamic agents, but, in addition to those, other processes and geohistorical factors have also intervened.

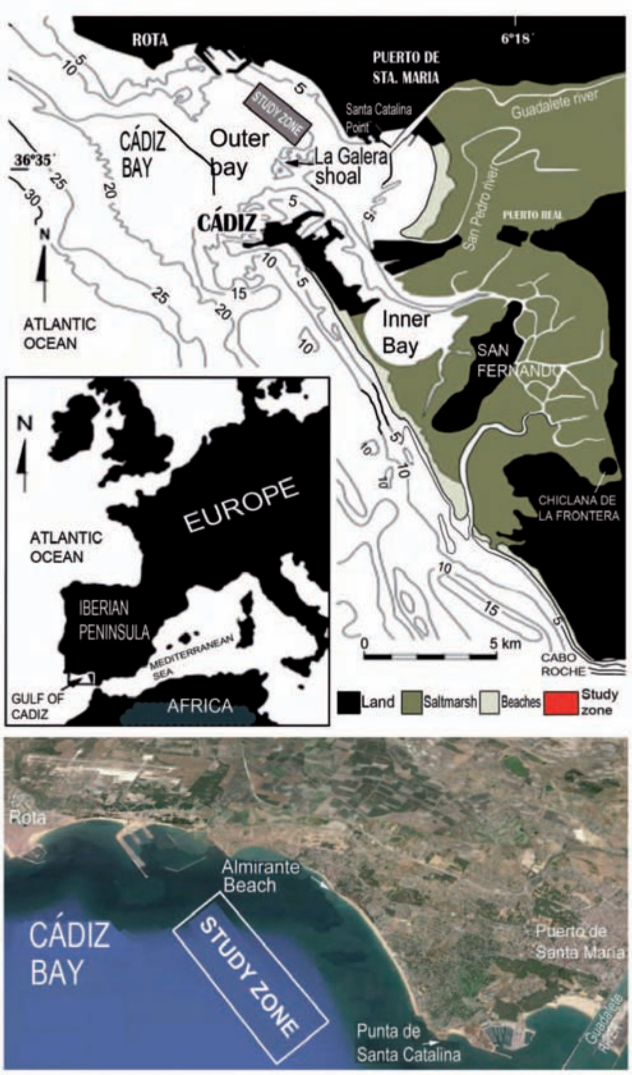

Fig. 1.- Location and aerial image of the study zone.

Geological setting

The study zone is located in the Gulf of Cadiz (SW Iberian Peninsula), in the subtidal zone of the Cádiz Bay, between Rota, Santa Catalina Point and the La Galera shoal, between 10 and 15 m in depth (Figs. 1 and 2). This zone is part of two geological realms: the Betic Mountain Range and the Guadalquivir basin (Fig. 2). During the Alpine orogeny, the push of the Mountain Range on the Paleozoic substrate formed the Guadalquivir foreland basin, where syn-orogenic diatomite marls were deposited from the Early to Late Miocene (Martín Algarra, 1987; Gutiérrez Mas *et al*., 1990; Sanz de Galdeano and Vera, 1992; López García, 1994, 1995; Berastegui *et al.*. 1998; Gutiérrez Mas *et al.*, 2009a, b; Gutiérrez Mas and Mas, 2013). A higher structural level is represented by post-orogenic sediments deposited in the Guadalquivir basin after the main tectonic stages of the Alpine Orogeny. These deposits are constituted of calcarenites, bioclastic sands and conglomerates (Gutiérrez Mas and Mas, 2013; González Acebrón *et al.*, 2016) (Fig. 2).

The neo-tectonic activity is important in the zone, being the outcrops affected by faults and tilts, resulting in a stepped coastline, controlled by NE-SW and NW-SE orientated fractures (Benkhelil, 1976; Gutiérrez-Mas and Mas, 2012). The coastal area is affected by diapiric elevations caused by Triassic gypsums, which are also recognizable in the continental margin, linked to transpressional transfers (Berastegui *et al.*, 1998; Sánchez-Guillamón, 2014; Vázquez *et al.*, 2015). Moreover, the zone is close to the Azores fault, limit between the African and Eurasian plates, which has sufficient potential to cause earthquakes, such as the known Lisbon earthquake (1755), and the tsunami that followed, which ravaged the coast of Portugal and Western Andalusia (Udias *et al.*, 1976; Campos Romero, 1991; Maldonado *et al.*, 1999; Gutiérrez-Mas *et al.*, 2016).

From the Late Holocene to the present-day, the marine sedimentation was controlled by standard marine agents, such as the wave and tide action, climate and sea-level changes. Other control factors are the neo-tectonic activity and the action of very-high energy events, such as great waves caused by major storms and tsunamis (Gutiérrez Mas *et al.*, 2009a, 2016).

The hydrodynamic regime is controlled by the wind regimen, tidal currents and waves. The most frequent winds are from W and SW (Fig. 3), but the E winds are also frequent (Gutiérrez-Mas *et al.*, 2009b). The waves have seasonal character, prevailing those from the westerly component (Fig. 3). The significant wave height is 0.6–1 m, and the maximum wave height is 4 m. The *sea wave* comes from NW and WNW, causing flows toward the SE, while *swell waves* comes from W. The calms have a wave height lower than 0.25 m, and represent the 28.5% from the type *sea*, and the 79.54% from the *swell* (National Climatic Data Center in Asheville, North Carolina, USA; Waves ROM). With regard to the wave action, their depositional effects are evident through the presence of *sand ribbons* on sandy bottoms. These are formed by effect of the relaxation flows during major storms.

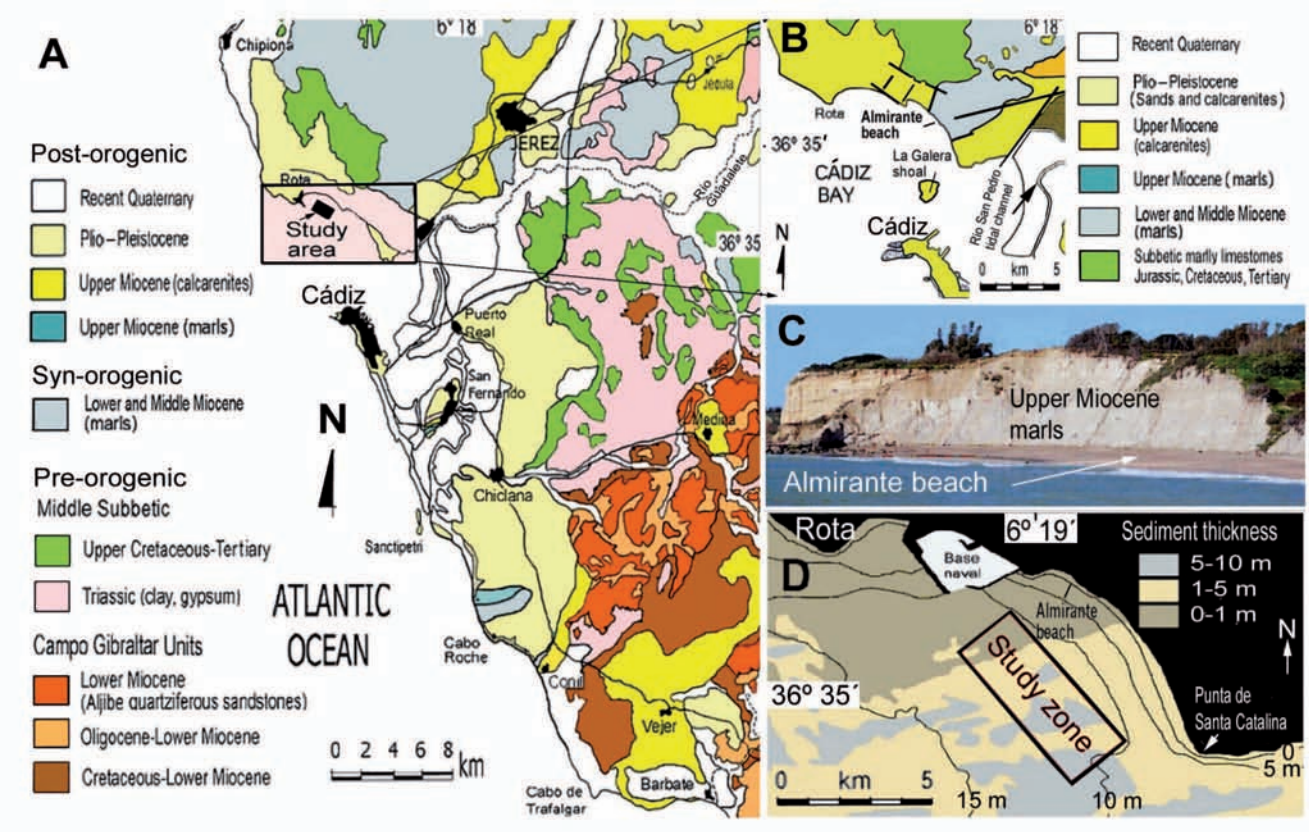

Fig. 2.- A) Regional geological map. B) Emerged outcrops close to the study zone. C) Image of Upper Miocene diatomite marls from the Almirante beach. D) Thickness distribution map of recent marine sediments.

The tides have semidiurnal character and mesotidal range, with a mean tidal range of 2.39 m and mean spring tidal range of 3.71 m**.** When the ebb reaches the Outer Bay, the presence on the bottom of the La Galera shoal, divides the tidal flow into two currents, one runs by the northern coast, while the other branch borders the Cadiz city toward the W and SW, following the coast physiography (Fig. 3C).

Material and methods

The study is based on the analysis of side scan sonar records, seismic profiles, and submarine sediment samples (Fig. 4). Geophysical study consisted of several campaigns of side scan sonar and seismic reflection profiles (3.5 kHz). Sonographic records were acquired from a Klein instrument, 3900 of high frequency (900 kHz) and 75 m of scan width. High resolution seismic profiles (3.5 kHz) were carried out to obtain information on the submarine substratum and sediment thickness, through a parametric mud penetrator, model SES-96 (Innomar Technologies GmbH), which had digitized data record, output power of 1–10 kW and transmission-reception frequency of 1–12 kHz.

Morphologic analysis was held from sonographic mosaics. Acoustic signals were digitally recorded for their processing and interpretation. Geometrical and morphological parameters, such as orientation, length and width of the bedforms were also measured.

Sediment samples were extracted through *van veen* dredge and gravity piston core. Sediment samples were positioned with Differential-GPS. The length of the piston cores was from 1.8 to 2 m; later these were cut, described, photographed and prepared for the grain size analysis. Grain size analysis was used to describe the facies and classify the de-

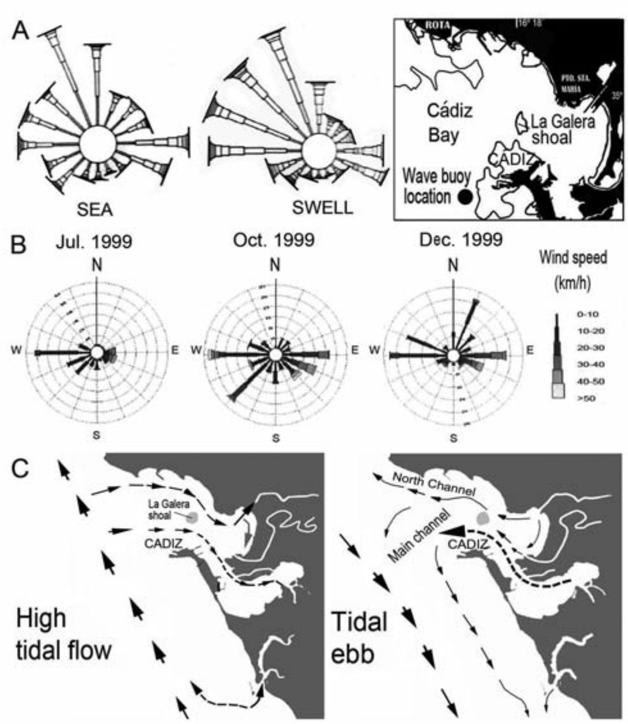

Fig. 3.- A) Wave height in deep waters. B) Wind diagrams in different periods. C) Tidal current directions (National Climatic Data Center in Asheville. North Carolina USA; Waves ROM).

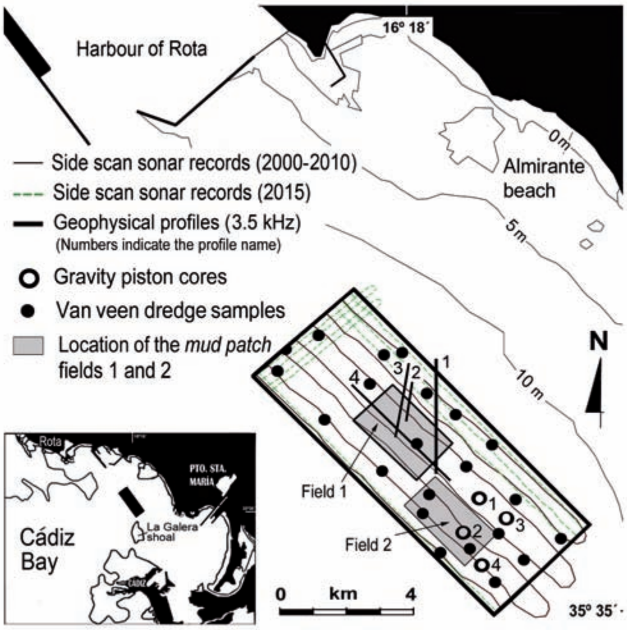

Fig. 4.- Location of the side scan sonar lines, seismic profiles and sampling stations.

posits. This was carried out by mechanical sieving to the coarse fraction (sand and gravel), and by via wet sieving to the fine fraction (silt and clay). Parameters and size grain distribution were also established. Microfossil content was observed through a binocular microscope.

Results

Sediment types

The bottoms from the Cádiz Bay are sandy although mud and gravel are also present (Fig. 5A). Rocky outcrops occupy an important part of the sea bottom and exert an important control on the currents and the sediment transport, and consequently on the sediment distribution. It is the case of the La Galera shoal (Figs. 1 and 3C), a Plio-Pleistocene outcrop that divides the ebb currents into two main flows or branches: one that runs along the northern edge of the bay, which is known as the North channel, and another that runs along the southern edge, bordering the city of Cádiz that is known as the Main channel.

The thickness of the non-consolidated sediments is variable with a range between 0 and 10 m and average thickness of 5 m (Fig. 2D). Between 0 and 10 m depth, the bottom is essentially rocky and sandy (Fig. 5A). The rocky bottoms correspond to Plio-Pleistocene outcrops, which are constituted of bioclastic gravels, sands, cemented calcarenites, and un-cemented bioclastic accumulations. At N and S from the La Galera shoal, there are fine sands, clay and sandy-clay (Fig. 5A). At W from La Galera shoal, between 10 and 15 m depth, the bottom sediments are sandy and sandy-clayey. In waters deeper than 15 m, this layout continues until the continental shelf is reached, where mud and clay are dominant.

Regarding the microfossil content of the marine sediments, both *van veen* dredge and cores samples show the presence of radiolarians, diatoms, planktonic and benthic foraminifers, and sponge spicules. Some foraminifers are similar to others found in recent sediments from the Cádiz Bay and adjacent continental shelf. However, radiolarians, diatoms and sponge spicules are similar to those found in marl outcrops from the Almirante beach cliffs, and whose ages range from the Tortonian to Messinian.

Submarine bedforms

The more frequent bedforms are *mud patches* and *sand ribbons* with superimposed *small ripple*s (Table I and Figs. 6, 7, 8), which are mainly located on muddy-sandy bottoms from 10 to 15 m depth (Fig. 9). However, some *sand ribbon* fields can reach until 30 m depth. At deeper than 30 m, in the inner continental shelf, the bottom is totally muddy and *mud patches* and *sand ribbons* are not observed.

Mud patches. The *mud patches* occupy a small part of the subtidal zone close to the Almirante beach (Figs. 4, 6,

Bedform types	Direction (Degrees)	Longitudinal axes (m)			Transverse axes (m)			Morphologies
		Max.	Mean	Min.	Max.	Mean	Min.	
Mud patches (subtidal zone)								
Field 1	N 200º- 230º	271.8	130	8.1	268.6	90	8.2	Lobed, Multilobed, Deltoid, Linguoid, Bilinguoid
Field 2	N 215º- 230º	86.3	40	8.1	100.3	30	6.1	Lobed, Multilobed Circular, Linguoid
Slides on continental Miocene diatomite marls								
Coastal cliff	N 200º-230º	131	100	72	145	75	7.1	Lobed, Linguoid, Deltoid
Sand ribbons (subtidal zone)								
Free sand ribbons	N 130º -140º	220	150	15	33	14	5	Elongated and straight
Sand ribbons embedded in mud patches	N 210 -230º	120	63	25	25	15	7.1	Curved and sinuous

Table I.- Geometrical parameters measured in bedform fields from the northern edge of the Cádiz Bay.

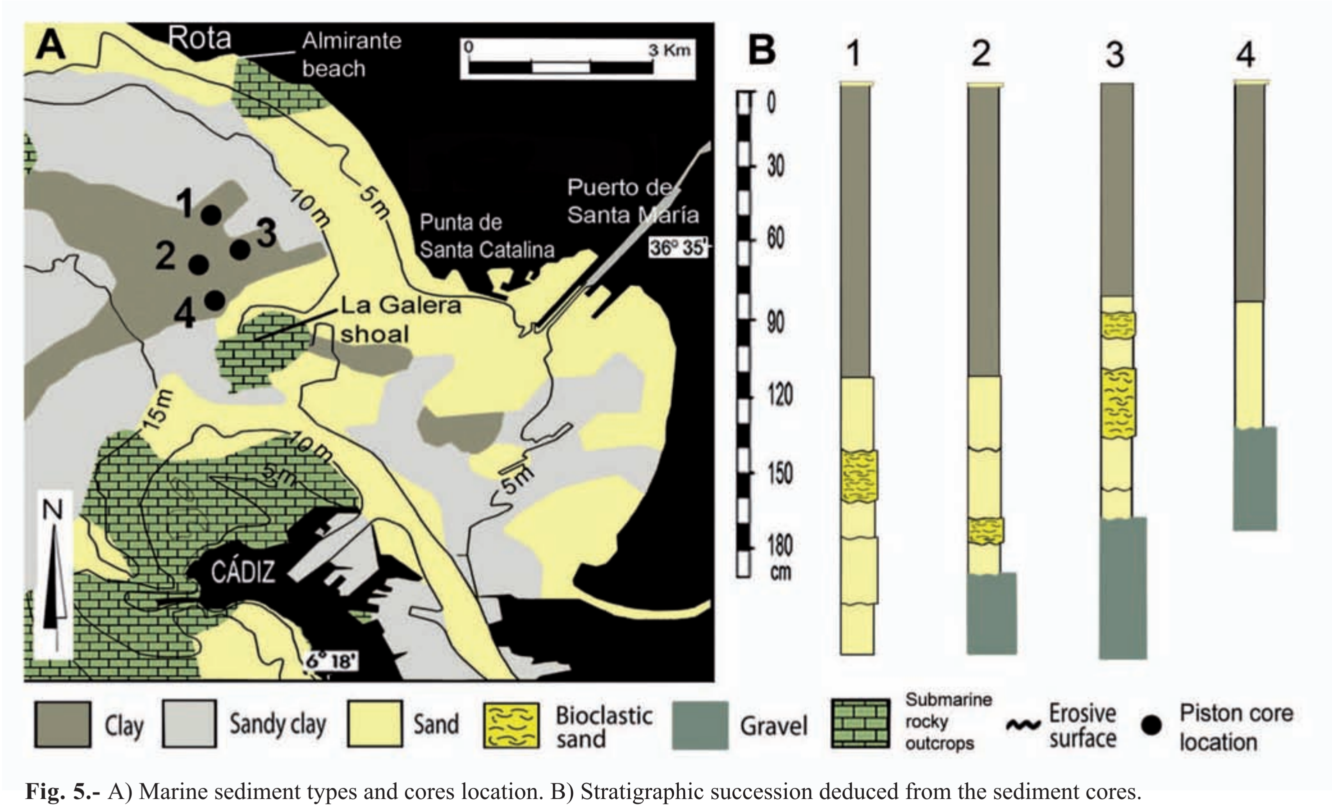

Fig. 5.- A) Marine sediment types and cores location. B) Stratigraphic succession deduced from the sediment cores.

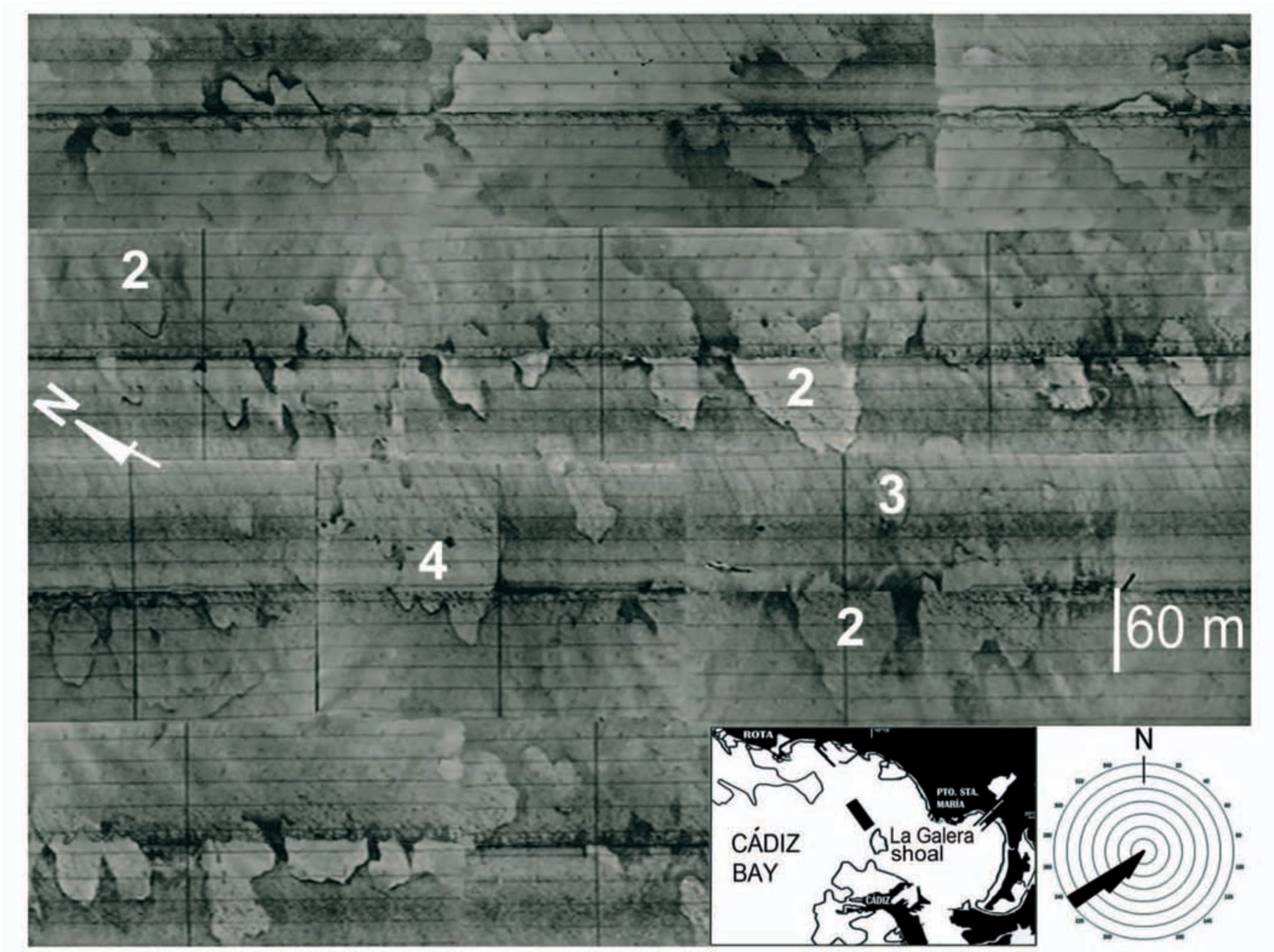

Fig. 6.- *Mud patches* from Field 1 (location in Fig. 4), and rose diagram showing longitudinal axe orientations. Legend: 1. Drag marks, 2. Linguoid *mud patches*, 3. Circular *mud patches*, 4. Multilobed *mud patches*.

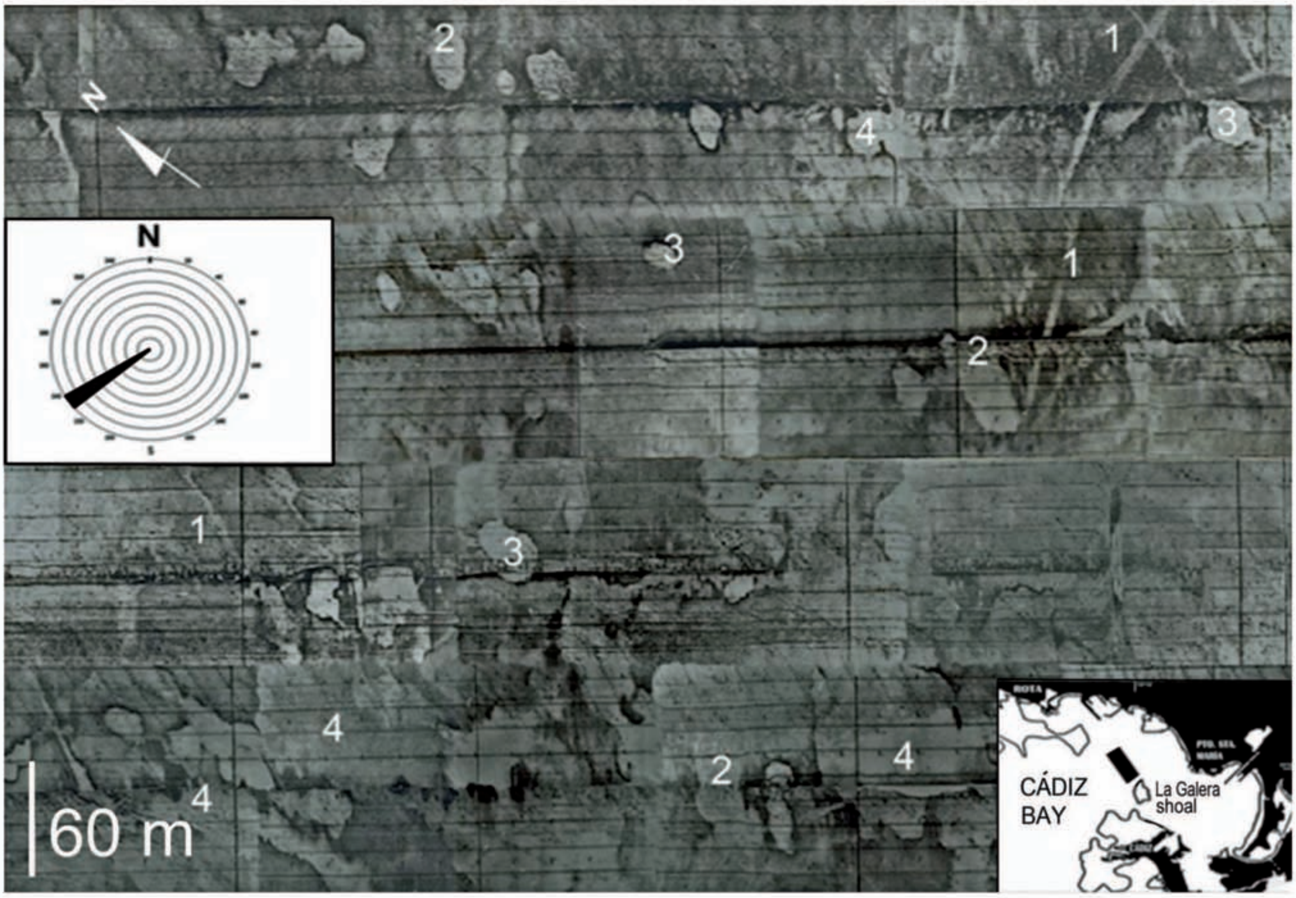

Fig. 7.- *Mud patches* from Field 2 (location in Fig. 4), and rose diagram showing longitudinal axe orientations. Legend: 1. Drag marks, 2. Linguoid *mud patches*, 3. Circular *mud patches*, 4. Multilobed *mud patches*.

7 and 8), which is the only zone of the Cádiz Bay where these morphologies are present. The *mud patches* are developed on muddy bottoms from 10 to 15 m depth. Their morphology is circular, oval, lingual, lobed and multilobed, and their longitudinal axes are SW orientated and reach up of 270 m long (Table I, Figs. 6, 7 and 8).

Two main *mud patch* fields are differentiated:

a) The Field 1 is located at NE of the study zone, between 10 and 15 m depth (Fig. 6). The sonar records show whitish patches, which correspond to little reflective sediments, such as mud or clay. These whitish patches are surrounded by darker greyish zones that correspond to reflective sediments, such as sands. The morphology is circular, lobed, and linguoid. The longitudinal axes are between 88 to 272 m length and SW oriented, and between 90 and 150 m wide (Table I). At NE the patches are greater and rounded, while at S these are smaller (120-170 m), but the longitudinal axes are also SW orientated.

b) The Field 2 is located on muddy bottoms, to depths between 13 and 14 m (Fig. 7). The dominant bedforms are cir-

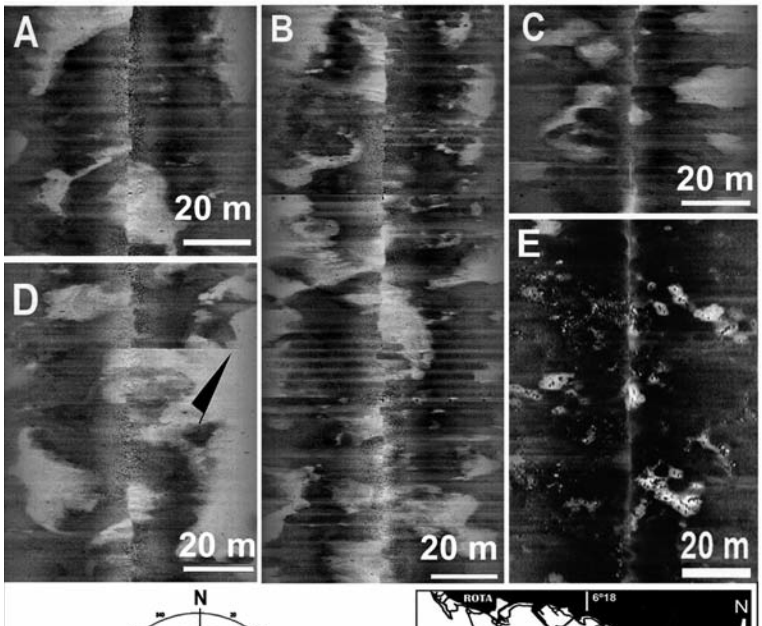

Fig. 8.- Recent sonographies (2015 AD), showing the permanence of the *mud patches*, and rose diagram displaying the orientation of the longitudinal axes.

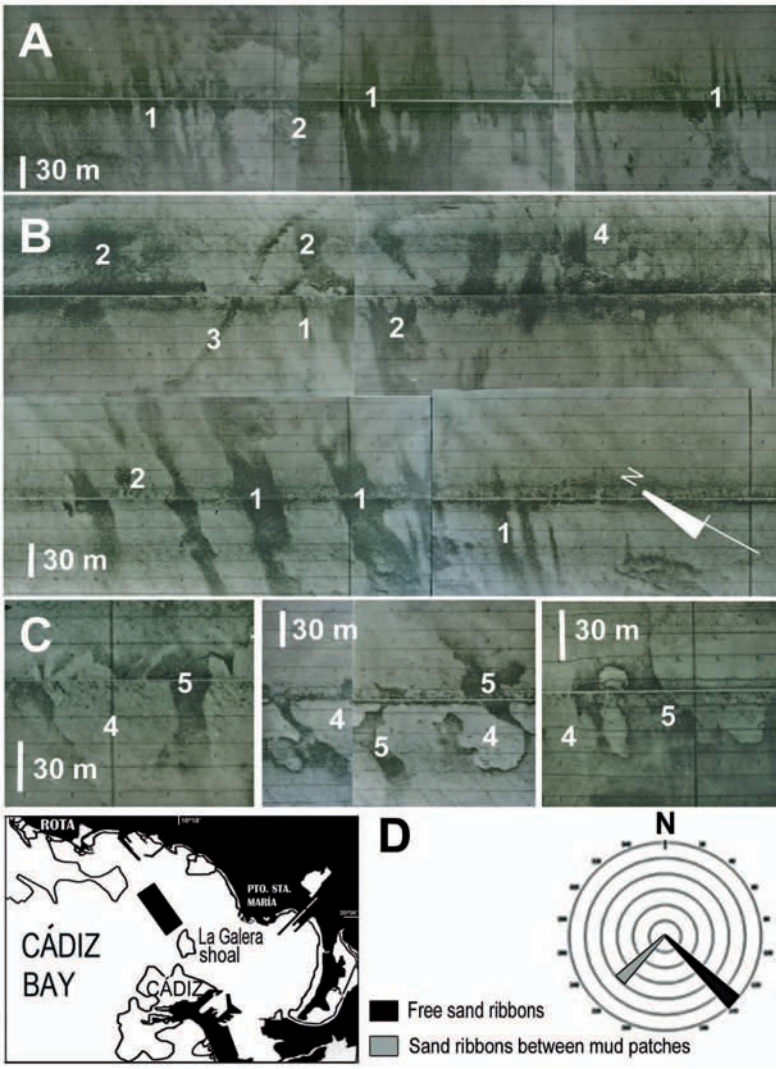

Fig. 9.- A and B) Free *sand ribbons*. C) *Sand ribbons* embedded in *mud patches*. D) Rose diagram showing the orientations of free *sand ribbons* and *sand ribbons* on *mud patches*. Legend: 1. Free *sand ribbons*, 2. *Sand patches*, 3, 4. *Mud patches*, 5. *Sand ribbons* embedded in *mud patches*.

cular and oval *mud patches*, with SW orientated longitudinal axes, and a similar size to those observed in the Field 1.

In order to verify the persistence over time of these *mud patches*, new side scan sonar records have been carried out (Fig. 8). The results indicate that the *mud patches* remain over time without major modifications and with a similar morphology, size and orientation to those observed in older sonographic records (Table I).

Sand ribbons. The *sand ribbon* fields are located on sandy bottoms between 10 and 15 m depth. By their elongated morphology and presence of superimposed *small ripples*, these bedforms are very remarkable in the sonar records (Fig. 9). Their origin is linked to directional flow action, such as the relaxation flows formed during major storms that are able to transport sand from the seashore toward deeper zones, where is deposited as *tempestites*. These show fining-upward sequences, with high-energy horizontal lamination, overlaid by cross lamination (Gutiérrez Mas *et al.*, 2009b).

Two types of *sand ribbons* are observed:

a) *Sand ribbons* on free sandy bottoms. These have rectilinear morphology and SSE orientation, according to the maximum slope direction on the bottom (Fig. 9A, B).

b) *Sand ribbons* embedded in *mud patches*. These are shorter than the free *ribbons*, and show curved paths with abrupt direction changes, because the morphologic control that the *mud patches* exert on the flows.

With regard to the seismic profiles (3.5 kHz) (Fig. 10), the results indicate that there is a relatively low acoustic penetration, because the existence of clay and/or liquefied gases, which cause acoustic shielding zones, that prevent the observation of deeper morphologies (Acosta Yepes, 1981; Parrado Román, 2000a), but it does not indicate anything about the *mud patches*.

Lateral and vertical variations are only observed in the profile tops, where the sedimentary sequence is constituted of an alternation of clay layers and fine sand layers. In regard to the *mud patches*, clayey deposits of similar morphology are recognizable in seismic profiles where the acoustic shielding zone is deeper, which is only observable in profiles parallel to the longitudinal axes of the *mud patches*, such as the profile 1 (Figs. 10B and C).

Although the acoustic shielding zones hardly reach up to 1 m under the bottom surface, this is enough to detect that the *mud patches* are located in places where the overlaying sandy layer is absent, which is coincident with the presence of small faults. These fractures can be outlet ducts to the underlying clay deposits, which appear over the surficial sands (Fig. 10C). These faults are also consistent with the position and orientation of escarpments located on the landslide heads.

With respect to the profile 4, which is perpendicularly orientated respect to the direction of the longitudinal axes of the patches, it did not provide information about the *mud patch* layout (Fig. 10A). The profile only shows the southern edge of the study zone, which is represented by La Galera shoal, an underwater Plio-Pleistocene outcrop which controls the tidal current directions, and the sediment distribution on the bottom (Figs. 3C and 5).

Marl outcrop from the Almirante beach

The coastal cliffs from the Almirante beach (Figs. 1, 2C and 11), indicate that the outcrops are constituted of white marls from the Upper Miocene, with thin sandy intercalations. The abundant microfossils, such as diatoms, radiolarian, sponge spicules, silicoflagellates, planktonic and benthic foraminifers, and ostracods, indicate a Tortonian-Messinian age.

Over the Upper Miocene marls, numerous landslides are observed (Fig. 11). These have variable morphology, but the circular, ellipsoidal and lobed forms are predominant (Fig. 11 and Table I). The longitudinal axes are between 72 and 131 m length, and their orientation is toward the WSW. Both, longitudinal axes and escarpments on the landslide heads, are controlled by ENE-WSW and ESE-WNW orientated fractures (Fig. 11C). The first direction corresponds to fractures perpendicular to the coastline, which also form grooves and small creeks. The second one corresponds to fractures parallel to the seashore, which control the coast dominant direction, and existence of stepped escarpments located on the landslide heads. A third structural direction is E-W which generates small grooves and escarpments that interfere with the previously described morphologies (Fig. 11).

Interpretation and discussion

The studied morphologies are not recognized in any other places of the sea bottoms from the Cádiz Bay, except in a small sectors from the study zone. It is therefore a singular case, reason why, in order to interpret the results and to establish the origin of these *mud patches*, two main issues should be considered: the depositional processes which caused the formation of the *mud patch* fields, and the provenance of the clay deposit on which these fields were developed.

Effect of tides and waves

The presence of *sand ribbons* on the sea bottom surface is an undoubted signal of an active sediment transport due to the directional flow action. These bedforms could be caused by relaxation flows generated by storm waves, combined effect of waves and tidal currents, or by action of greater waves caused by oceanographic events. The *sand ribbons* occur by shear effect of the current on the bottom sediments (Álvarez *et al.*, 1997), and subsequent transport and deposition of sand. The question is to establish if these flows are also able to form *mud patches* of morphology, size and orientation similar to those observed in the sonographic records.

In order to establish the wave and tide effect on the bottom sediments, Álvarez *et al.* (1997) elaborated a high-resolution hydrodynamic model for the Cádiz Bay, which simulates different hydrodynamic situations. An interesting situation is that in which the wave and tide effects are attached. The analysis of the variability of the drag coefficient (stress over seabed) and the energy dissipation, representative of the current influence on the sediment load during a tidal cycle, shows an increase of the drag coefficient in shallow bottoms of the Puntales Strait (Fig. 12), where a decrease of the current speed of 4–8 cm/s is observed, while in shallower bottoms of the Bay the decrease is only of 2–4 cm/s (Kagan *et al.*, 2001, 2005). The data indicates that, if the wave and tide effects are attached, the maximum current speed occurs in a waters deeper than that existing in the study zone, because in shallow bottoms the energy of the flow is balanced with the dissipation of the tidal energy over the bottom (Fig. 12). So, it must be considered that the combined effect of waves and tides is not significant in the zone where the *mud patches* are located. The resulting currents are not enough strong to generate bedforms of morphology and size similar to the *mud patches* observed in the sonagraphic records.

According to the model of Coleman and Prior (1981), the clayey landslides were deposited above a thin layer of sand, after that this was broken by the displacement of the underlying mud, resulting in a *mud patch* field, such as it is seen in the side scan sonar records, where the patches (whitish colour) are surrounded by sand (dark gray tones) that remained unbroken on the sea bottom. However, the data indicate that the combined effect of waves and tides are not the triggering factor of the process.

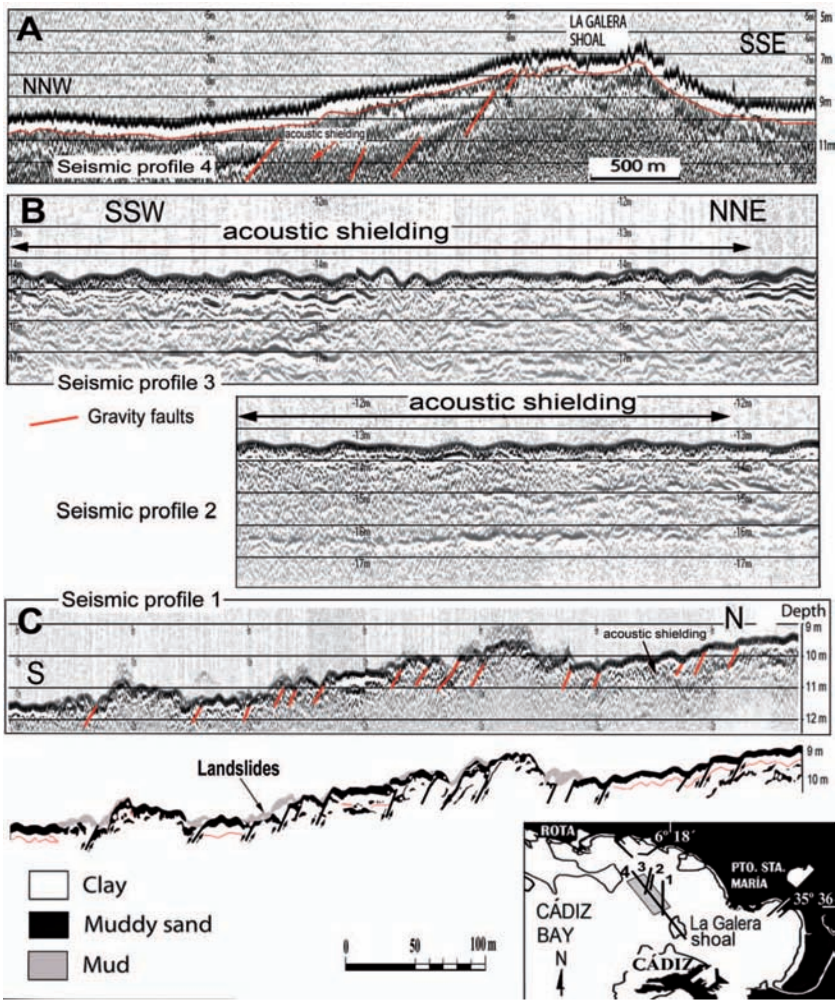

Fig. 10.- Seismic profiles (3.5 kHz), and their location on the study zone.

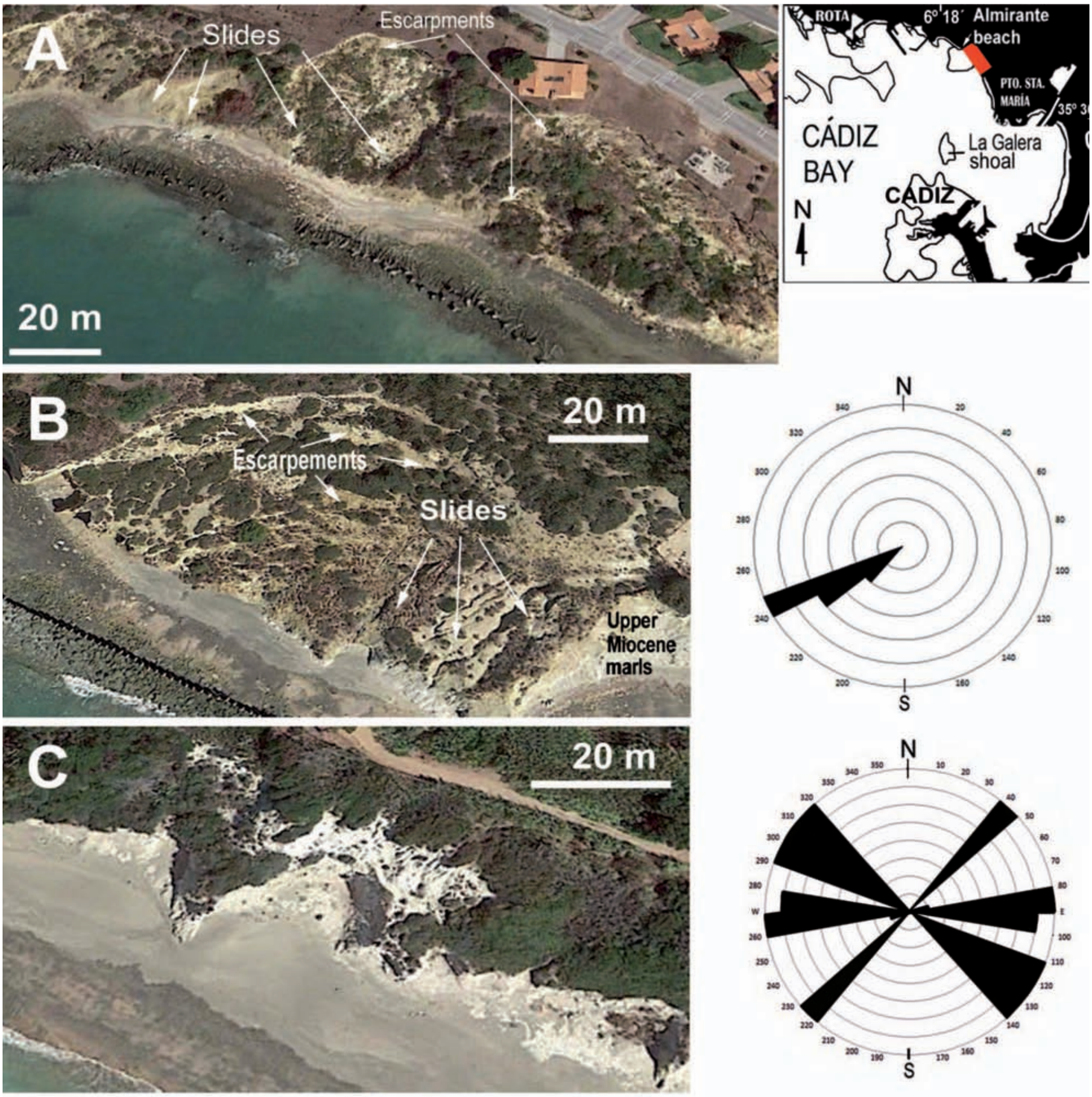

Fig. 11.- A) Aerial image of the Almirante beach, showing landslides on diatomite marls. B) Aerial image of circular and lobed landslides, and rose diagram showing longitudinal axe orientations. C) Coastline variations linked to different fracture directions in the Almirante beach, and rose diagram showing the main structural directions.

On the other hand, as previously commented, a sand active transport from the shore to offshore is evidenced by the presence of *sand ribbons* fields (Fig. 13). In this sense, the presence on the sea bottom of different typologies, indicates a differentiated hydrodynamic and depositional behavior. On free bottoms, where there are no *mud patches* or rocky outcrops, the *sand ribbons* are straight and orientated according to the maximum slope direction, that is, toward the SE (Fig. 13D). However, on bottoms where there are *mud patches* fields, the *sand ribbons* paths show different orientations, since the flows are driven by the grooves between *mud patches*, according to the dominant direction of these toward the SW (Fig. 13D).

Thereby, the different orientations of the *sand ribbons* developed on free bottoms and the *sand ribbons* embedded in *mud patches*, confirm that the action of the operant flows in the study area, are not able to form *mud patches*, but rather waves and tides, even the combined effect of both, have limited their action to a partial remobilization of preexisting deposits, so that other factors and processes must be investigated.

Event action

With regard to event action, such as earthquakes and tsunamis, historic events are cited in the Cádiz coast, such as the Lisbon earthquake of 1755 yr. AD, and the tsunami that followed, which had devastating effects on the Andalusia Atlantic coasts (Udias *et al.*, 1976; Grimison and Chen, 1986, 1988; Campos Romero, 1991; Dawson *et al.*, 1995;

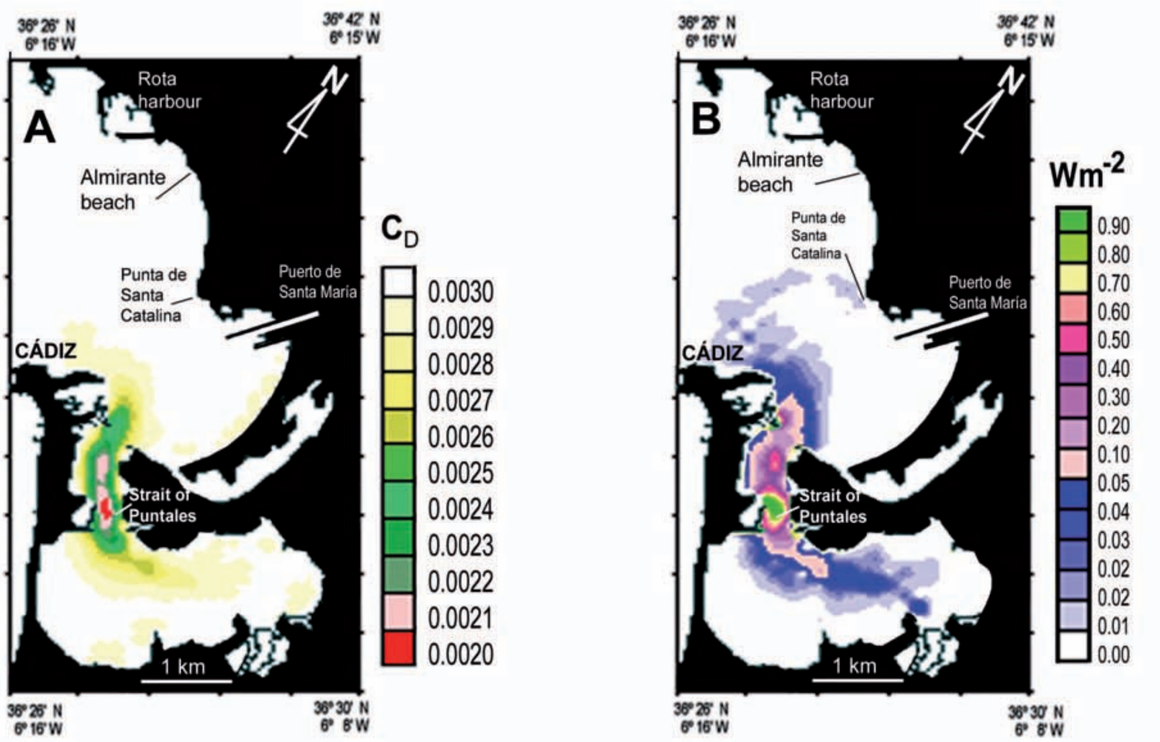

Fig. 12.- Relations between tidal currents and bottom sediment mobility. A) Mean (over a mean tidal cycle) drag coefficient (CD) predicted with allowance for sediment load effect. B) Mean (over a tidal cycle) energy dissipation, Wm^{-2}. (Modified from Álvarez *et al.*, 1999).

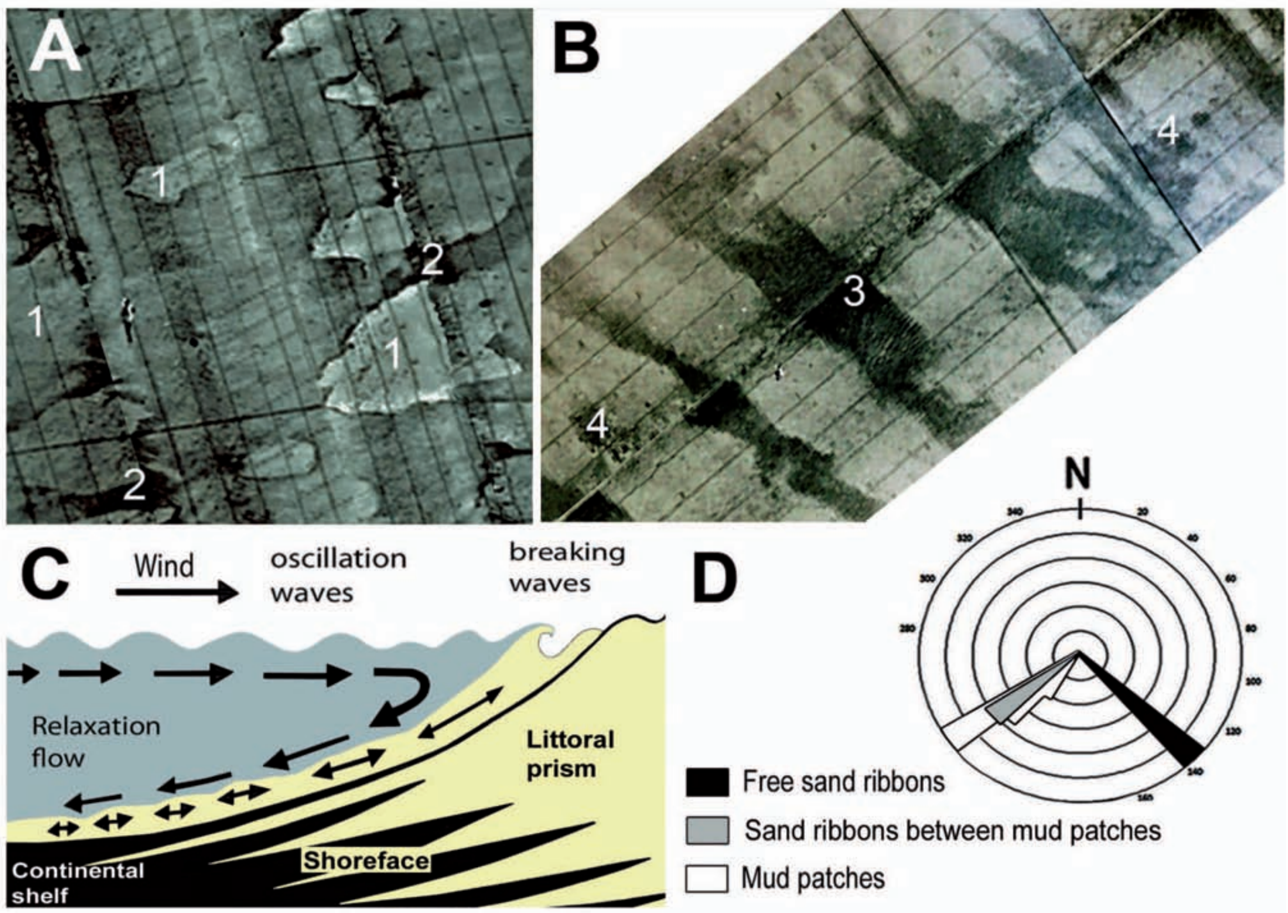

Fig. 13.- A) Sonographic image of *sand ribbons* (2) embedded in *mud patches* (1). B) Free *sand ribbons* (3) and *sand patches* (4). C) Relaxation flows caused by storm waves, and deposits of tempestites on the shoreface. D) Rose diagram showing the orientations of free *sand ribbons* respect to *sand ribbons* embedded in *mud patches.*

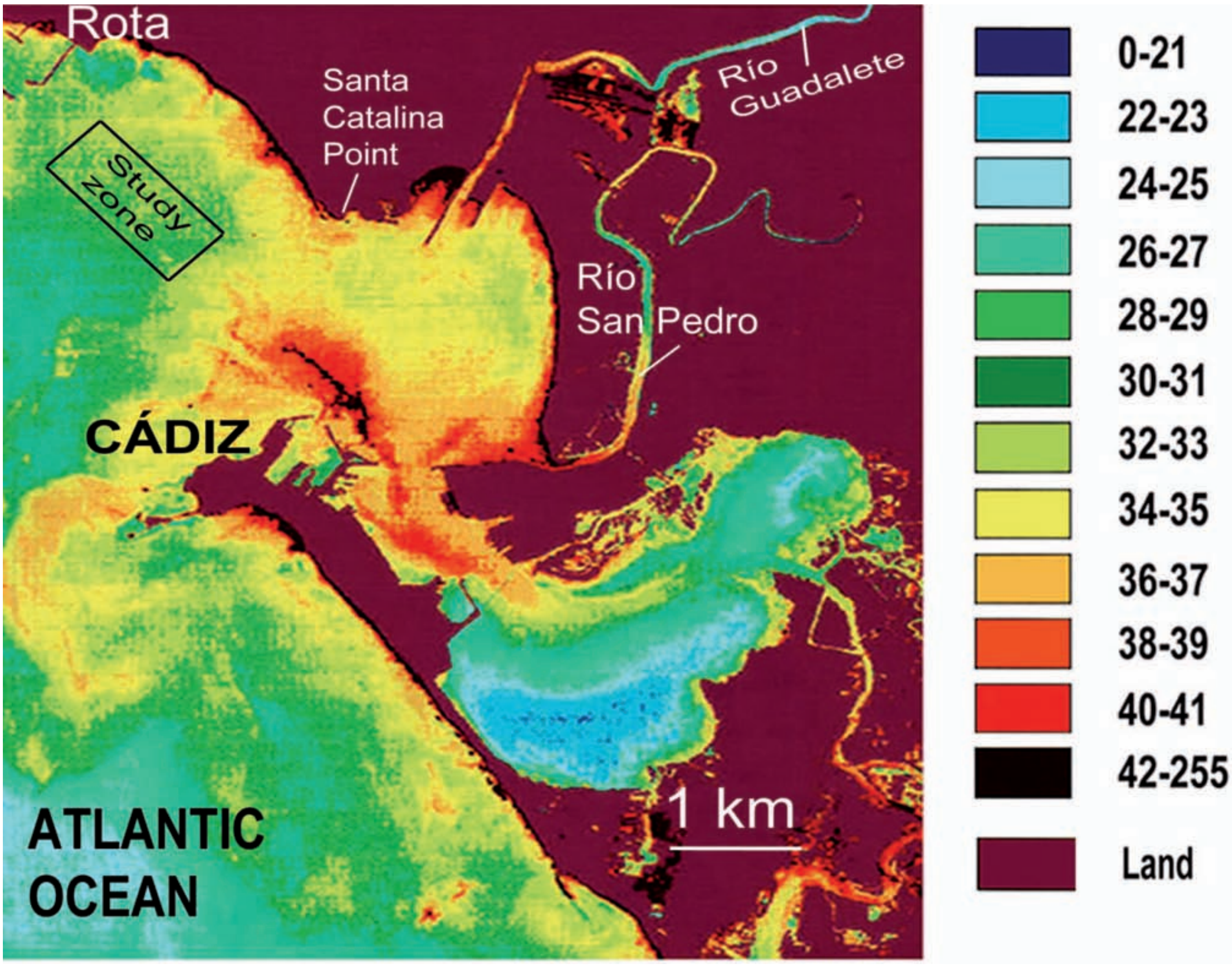

Fig. 14.- Landsat image of suspended matter flows in the Cádiz Bay. Values of DM (Digital Numbers), Tide height: 2.56 m, Wind speed: calm. (Andalucía Environmental Agency).

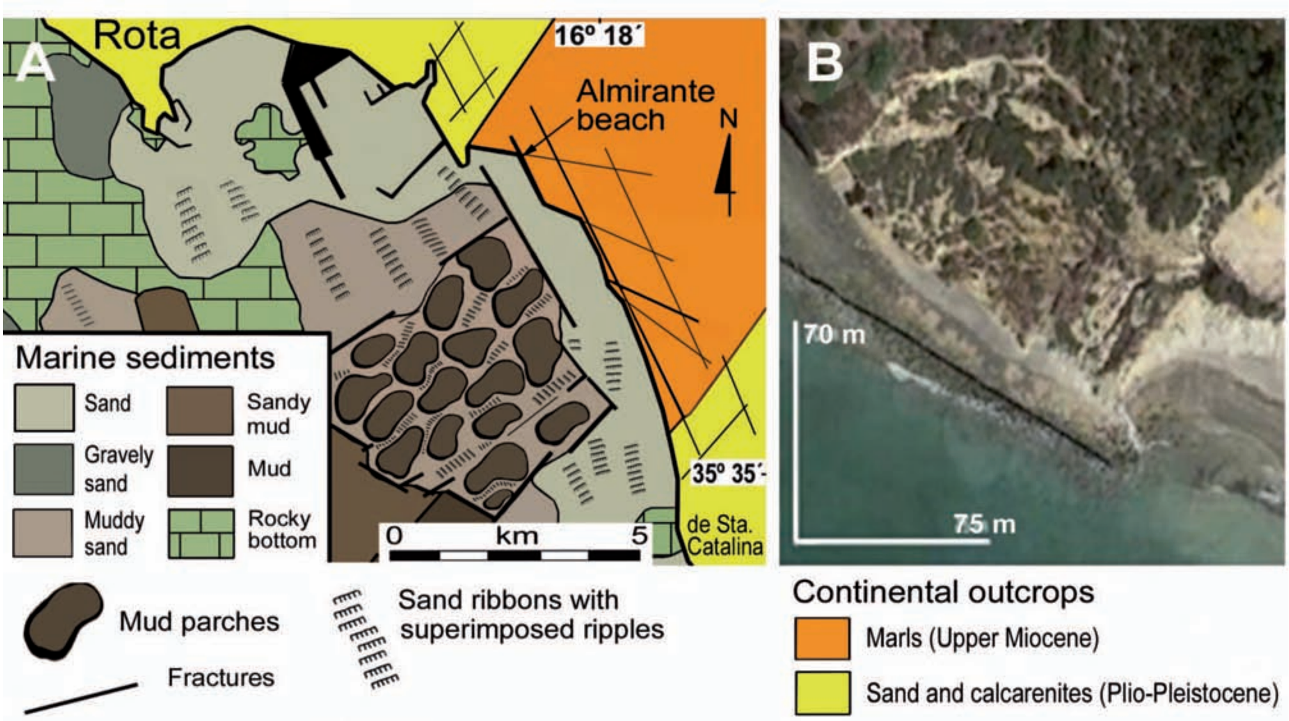

Fig. 15.- A) Geological map of the Almirante beach and nearby subtidal zone. B) Aerial image of the Almirante beach and landslides development on Miocene diatomite marls.

Baptista *et al.*, 1998; Borja *et al.*, 1999). In this sense, if the wave height assigned to the cited tsunami is considered, the earthquake magnitude correspond to 4.5 degrees in the Tsunami Japanese Scale (Iida, 1963a, b), which is equivalent to an earthquake of 8.5–9 degrees in the Richter scale (Campos Romero, 1991). However, if the bottom physiography effect is considered, the earthquake magnitude should be lower, although enough to cause the devastation of the coastal areas. From the depth and distance to the coast, the sea bottoms of the study zone should be intensely affected by both earthquake and tsunami (Gutierrez Mas *et al.*, 2016).

The earthquake action could be by cutting effect of the seismic waves on the bottom, which causing instability of the sediments, an increase of the pressure on the sediment granular pores, the liquefaction of hydrated-gas present in the deposits and gas scape. The presence of hydrated gases in submarine deposits is an important mechanism to cause submarine landslides (Hampton *et al.*, 1996; Kvenvolden, 1995, 1998; Gardner *et al.*, 1999). Earthquakes and tsunamis can change the mechanical properties of the sediments, transforming them in a solid of lower volume and permeability, which facilitates the gas escape and the rupture of the overlaying sediments (Pecher *et al.*, 2004). On the other hand, the existence of faults of small slump could also facilitate the exit of clay toward the sea bottom surface.

Regarding to the direct effects of the tsunami, the great waves must generate up-run and upward currents, as well as the dragging of a great quantity of sediments, which were transported and deposited on the shore and even inland. Later, the sediments were transported seaward and deposited on the shoreface as *sand ribbons* (Fig. 13), and on the inner continental shelf as *tempestites.*

Given the location of the study area, it is undoubted that these processes could occur. However the depositional effects of both earthquake and tsunami did not reach beyond producing erosion and remobilization of pre-existent deposits, as well as the formation of *sand ribbon* fields to different depths and distances from the coast. But it does not mean that the tsunami waves caused the *mud patch* fields, since these bedforms are only located in a small sector of the Cádiz Bay. If the *mud patches* were caused by the 1755 AD tsunami, similar bedform fields would be widely spread on the bottoms of the Cádiz Bay.

Provenance of the clay deposits

Two possibilities are discussed:

a) The clays were provided by the action of the standard marine agents and deposited from the suspension. The main sources of suspended matter to the Outer Bay are the Guadalete River mouth, the Río San Pedro tidal channel, and the Puntales Strait (Guillemot *et al.*, 1987; Gutiérrez Mas *et al.*, 2006). The paths of the tidal flows transporting suspension matter are marked on the seabed. Fine sediments, such as mud and sandy mud, are deposited on the seabed forming bands that follow the trajectories of the currents (Fig. 5).

The suspended matter flumes that circulate in the Cádiz Bay follow the same paths that the tidal currents essentially the ebb. The flow directions detected from Landsat satellite images (Fig. 14), indicate that the study zone is located in a place where the concentration of suspended matter in sea water is low, from 24 to 30 mg/l to calm conditions. Under these conditions, the arrival of suspended matter to the zone is minimum, while the clay sedimentation rate on the sea bottom is also low. The facts suggest that the clay deposits on which the *mud patches* fields are located are not a consequence of the current marine dynamics.

b) The clay deposits on which the *mud patches* are developed correspond to older outcrops that currently are submerged. Aerial images of the coastal cliffs from the Almirante beach show the existence of landslides development on Miocene white marls (Fig. 14 see pag. 51, Table I). These landslides have morphologies, size and direction similar to the *mud patches* observed in the close subtidal zone. These marls contain diatoms and radiolarians that also are recognized in some underwater samples, although these are mixed with remains of younger marine organisms.

According to these data, the *mud patches* fields could correspond to inherited morphologies from an older outcrop, similar to those present in the coastal cliff from the Almirante beach, which are currently submerged and subjected to reworking by the current hydrodynamic agents.

The neo-tectonic activity is also important in the evolution of these outcrops, since faults and fractures are responsible of the distribution of emerged and submerged zones (Figs. 11C and 15, see pag. 51). Fractures oriented from NE to SW are responsible of the size and orientation of the longitudinal axes of the *mud patches*, while the fractures oriented from NW to SE are responsible of the directions of the escarpments located on the landslides head.

Conclusions

The data about submarine landslides in shallow sea beds from the Cádiz Bay are scarce, because these morphologies are uncommon or have not yet been detected. However, in a small sector located in the subtidal zone from the northern edge of the Bay, several *mud patch* fields have been observed in side scan sonar records. These morphologies appear as whitish patches surrounded by dark-grey sand. These patches were initially interpreted as underwater landslides, and their origin attributed to the marine agent action on a muddy-sandy bottom, according to the Coleman and Prior (1981) model.

A critical review carried out on older data, together to results provided by new investigations, indicate that the presence of these *mud patches* is not only a consequence of the hydrodynamic agents. Regular tidal and waves are not capable of causing these morphologies. Geometric parameters measured in the underwater *mud patches*, indicate that there is no relationship between these and the direct action of the waves and tides.

The geophysical data show the existence of normal faults of small slump, which broke the sea bottom surface and the sandy layer located at sequence top, facilitating the exit of the clayey deposits. Hydrated gas scape, major storms, earthquakes and tsunamis, could cause the reactivation of these bedforms, but they were not either cause of their formation.

A significant fact is that these morphologies are not recognized in any other places of the Cádiz Bay, which means that the factor controlling their existence have a local character. The geometric parameters measured in the underwater *mud patches*, are similar to landslides developed on Miocene diatomite marls from the Almirante beach. The data indicate that the *mud patch* fields represent the continuity seaward of the marl outcrop present in the coastal cliff, and that the *mud patches* are also landslides. Both emerged and underwater outcrops show numerous lobed morphologies caused by surficial erosion and gravity slides, in a terrestrial environment, before the sea reached its current level.

The combined effect of the tectonic structure, little compacted deposits, together the current sea-level position, justifies the existence of these underwater *mud patches* fields. Later these outcrops were submerged, and the marls underwent reworking and re-sedimentation processes by major storms, earthquakes and tsunamis, which also cause gas scape and even reactivation of the displacement processes.

Acknowledgments

This paper has been supported by the Research Project GL2010-16878 from the Ministry of Science and Innovation of Spain (FEDER). We also thank to the Instituto Hidrográfico de la Marina for its collaboration, as well as to the D[ra] Belén Alonso and to the Journal Editor for their invaluable corrections, advice, and suggestions.

References

Acosta Yepes, J. (1981): Apantallamientos acústicos en la ría de Muros y Noya y en el margen continental de Cádiz. *Boletín del Instituto Español de Oceanografía*, Vll (1): 126–149.

Álvarez, O., Tejedor, B. and Tejedor, L. (1997): Simulación hidrodinámica en el área de la Bahía de Cádiz. Análisis de las constituyentes principales. In: *IV Jornadas Españolas de Ingeniería de Puertos y Costas*. Servicio de Publicaciones de la Universidad Politécnica de Valencia 98. 2125: 125–136.

Álvarez, O., Izquierdo, A., Tejedor, B., Mañanes, R., Tejedor, L., and Kagan, B.A. (1999): The influence of sediment load on tidal dynamics, a case study: Cádiz Bay. *Estuarine, Coastal and Shelf Sciences*, 48: 439–450.

Baptista, M.A., Miranda, P.M.A., Miranda, J.M. and Mendes Victor, L. (1998): Constrains on the source of the 1755 Lisbon tsunami inferred from numerical modelling of historical data on the source of the 1755 Lisbon tsunami. *Journal Geodynamics*, 25 (2): 159–174.

Benkhelil, J. (1976): Etude néotectonique de la terminason occidentale des Cordilleres Betiques (Espagne). Tesis doctoral. Univ. Niza. 180 p.

Berastegui, X., Banks, C., Puig, C., Taberner, C., Waltham, D. and Fernández, M. (1998): Lateral diapiric emplacement of Triassic evaporites at the southern margin of the Guadalquivir Basin, Spain. In: *Cenozoic foreland basins of Western Europe*, (A. Mascle, C. Puig de Fábregas, H.P. Luterbacher and M. Fernández M, Eds), *Geological Society, Special Publication*, 134: 49–68.

Borja, F., Zazo, C., Dabrio, C.J., Díaz del Olmo, F., Goy, J.L. and Lario, J. (1999): Holocene aeolian phases and human settlements along the Atlantic coast of Southern Spain. *The Holocene*, 9: 333–339.

Campos Romero, M.L. (1991): Tsunami hazard on the Spanish coasts of the Iberian Peninsula. *Science of Tsunami Hazards*, 9: 83–90.

Coleman, J.M. and Prior, D.B. (1981): Subaqueos sediment instabilities offshore Mississippi River Delta. In: *Offshore Geologic Hazards*, AAPG Educational Course, Notes Series, 18: 1–53.

Dawson, A.G., Hindson, R., Andrade, C., Freitas, C., Parish, R. and Bateman. M. (1995): Tsunami sedimentation associated with the Lisbon earthquake of 1 November AD 1755: Boca do Rio, Algarve, Portugal. *The Holocene*, 5: 209–215.

Garcia-Castellanos, D., Estrada, F., Jiménez-Munt, I., Gorini, C., Fernández, M., Vergés, J. and De Vicente, R. (2009): Catastrophic flood of the Mediterranean after the Messinian salinity crisis. *Nature*, 462 (7274): 778–781.

Gardner, J.V., Prior, D.B. and Field, M.E. (1999): Humboldt Slid – a large shear-dominated retrogressive slope failure. *Marine Geology*, 154: 323–338.

González-Acebrón, L., Mas, R., Arribas, J., Gutiérrez-Mas, J.M. and Pérez-Garrido, C. (2016): Very coarse-grained beaches as a response to generalized sea level drops in a complex active tectonic setting: Pleistocene marine terraces at the Cadiz coast, SW Spain, *Marine Geology*, 382: 99–110.

Grimison, N.L. and Chen, W.P. (1986): Earthquakes in the Davie Ridge-Madagascar region and the southern termination of the African-Somalian plate boundary. *Eos, Transactions, American Geophysical Union*, 67 (44): 1105.

Grimison, N.L. and Chen, W.P. (1988): Source mechanisms of four recent earthquakes along the Azores–Gibraltar plate boundary. *Geophysical Journal of the Royal Astronomical Society*, 92: 391–401.

Guillemot, E. (1987): Télédétection des milieux litoraux de la baie de Cadix. Doctoral thesis. Univ. Paris, 146 p.

Gutiérrez Mas J.M., Martín Algarra A., Domínguez Bella S. and Moral Cardona J.P. (1990): *Introducción a la Geología de la provincia de Cádiz*. Servicio de Publicaciones. Universidad de Cádiz. 315 p.

Gutiérrez-Mas, J.M., Lopez-Aguayo, F. and Achab, M. (2006): Clay minerals as dynamic tracers of suspended matter dispersal in the Gulf of Cadiz (SW Spain). *Clay Minerals*, 41: 727–738.

Gutiérrez-Mas J.M., Juan C. and Morales J.A. (2009a): Evidence of high energy events in shelly layers interbedded in coastal Holocene sands in Cadiz Bay (south-west Spain). *Earth Surface Processes and Landforms*, 34: 810–823.

Gutiérrez-Mas, J.M., López-Arroyo, J. and Morales, J.A. (2009b): Recent marine lithofacies in the Cadiz Bay (SW Spain). Sequences, processes and control factors. *Sedimentary Geology*, 218: 31–47.

Gutiérrez-Mas, J.M. and Mas J.R. (2012): Pliocene lithofacies within the marine geologic record from the Cadiz Bay (SW Spain): environments and processes. *Revista de la Sociedad Geologica de España*, 25 (3-4): 119–132.

Gutiérrez-Mas, J.M. and Mas, J.R. (2013): Record of very high energy events in Plio-Pleistocene marine deposits of the Gulf of Cadiz (SW Spain): facies and processes. *Facies*, 59: 679–701.

Gutiérrez-Mas J.M., Morales J, A. and Delgado, I. (2015): Respuesta morfo-sedimentaria de alta energía en el fondo de un delta de reflujo mareal en la desembocadura del Canal de Sanctipetri (Bahía de Cádiz, SO España). *Revista de la Sociedad Geologica de España*, 28(1): 105–117.

Gutiérrez-Mas, J.M., Gómez Fernández, V., García-López, S., Morales, J.A. and Ibáñez Ageitos, J.M. (2016): Comparative analysis of the deposits left by the tsunami that followed to the Lisbon earthquake (1755 ad), on the Castilnovo beach and the old tuna factory of la Chança (Conil de la Frontera, SW Spain). *Revista de la Sociedad Geologica de España*, 29 (1): 21–33.

Hampton, M.A., Lee, H.J. and Locat, J. (1996): Submarine landslides. *Reviews of Geophysics*, 34: 33–59.

Iida, K (1963a): Magnitude, energy, and generation of and mechanisms of tsunamis and a catalogue of earthquakes associated with tsunamis. *Proc. Tsunami Meetings Associated with the Tenth Pacific Science Congress*. Monograph No. 24. IUGG, 167–173.

Iida, K. (1963b): On the estimation of tsunami energy. *Proc. Tsunami Meetings Associated with the Tenth Pacific Science Congress*. Monograph No. 24. IUGG, 7–18.

Kagan, B.A., Tejedor, L., Alvarez, O., Izquierdo, A., Tejedor, B. and Mananes, R. (2001): Weak wave-tide interaction formulation and its application to Cadiz Bay. *Continental Shelf Research*, 21: 697–725.

Kagan, B.A., Alvarez, O. and Izquierdo, A. (2005): Weak wind-wave/tide interaction over fixed and moveable bottoms a formulation and some preliminary results. *Continental Shelf Research*, 25: 753–773.

Kvenvolden, K. (1995): A review of the geochemistry of methane in natural gas hydrate. *Organic Geochemistry,* 23: 997–1008.

Kvenvolden, K. (1998): A primer on the geological occurrence of gas hydrates. In: *Gas hydrates - Relevance to World Margin Stability and Climate Change*: (J.P. Henriet and J. Mienert, Eds.), *The Geological Society, Special Publication*, 137: 9–30.

Lobo, F.J., Hernández-Molina, F.J., Somoza, L., Rodero, J., Maldonado, A. and Barnolas, A. (2000): Patterns of bottom current flow deduced from dune asymmetries over the Gulf of Cadiz shelf (southwestern Spain). *Marine Geology*, 164: 91–117.

López García, M.J. and Bustillo, M.A. (1994): Los sedimentos con diatomeas del mioceno en la Cuenca del Guadalquivir: edad y composicion litológica. *Estudio Geológicos*, 50: 71–90.

López García, M.J. (1995): Resultados paleoceanograficos deducidos a partir del contenido en diatomeas de los sedimentos siliceos miocenos (moronitas) en la Cuenca del Guadalquivir. *Estudios Geológicos,* 51: 29–41.

Maldonado, A., Somoza, L. and Pallares, L. (1999): The Betic Orogen and the Iberian-African boundary in the Gulf of Cadiz: geological evolution. *Marine Geology*, 155: 9–43.

Martin-Algarra, A. (1987): Evolución geológica alpine del contacto entre las Zonas Internas y las Zonas Externas de la Cordillera Bética. Tesis Doctoral, Univ. Granada, 1171 p.

Pajarón, L., Fernández-Puga, M.C., Vazquez, J.T. and Fernández Salas, L.M. (2015): Characterization of submarine slides in the upper and middle slope of the Gulf of Cadiz (SW Iberian Peninsula). Summaries of the VIII Symposium MIA, Malaga (Spain). 173–176.

Parrado Román, J.M., Gutiérrez Mas, J.M., Jodar Tenor, J.M., Luna del Barco, A. and Achab, M. (2000a). Interpretation and evolution of muddy patches in the northern sector of the Bay of Cadiz. *Geo-Temas*, 1(4): 197–202.

Parrado Román, J.M., Gutiérrez Mas, J.M., Luna del Barco, A., Jodar Tenor, J.M. and Achab, M. (2000b). Clasificación del régimen de flujo en la bahía de Cádiz a partir del análisis de formas de fondo. *Geogaceta*, 27: 131–134.

Pecher, I.A., Henrys, S.A. and Zhu, H. (2004): Seismic images of gas conduits beneath vents and gas hydrates on Ritchie Ridge, Hikurangi Margin, New Zealand. , 47: 275–279.

Sánchez-Guillamón, O., Vázquez-Garrido, J.T., Fernández-Puga M.C., Fernández-Salas, L.M. and Díaz del Rio V. (2014): Characterization of active normal faults in the Gulf of Cádiz continental shelf (SW Iberian Peninsula). *Summaries of the Second Symposium on active faults and paleoseismology*. Lorca (Spain): 129–132.

Sanz de Galdeano, C. and Vera, J.A. (1992): Stratigraphic record and palaeogeographical context of the Neogene basins in the Betic Cordillera, Spain. *Basin Research*, 4: 21–36.

Somoza, L., Hernández-Molina, F.J., De Andrés, J.R. and Rey, J. (1997): Continental shelf architecture and sealevel cycles: Late Quaternary high-resolution stratigraphy of the Gulf of Cádiz, Spain. *Geo-Marine Letters,* 17: 133–139.

Udías, A., López-Arroyo, A. and Mezcua, J. (1976): Seismotectonic of the Azores-Alborán región. *Tectonophysics*, 31: 259–269.

Vázquez, J.T., Fernández-Puga, M.C., Palomino, D., Fernández-Salas, L.M., Sánchez-Guillamón, O., López-González N., Díaz del Río V. and Vegas, R. (2015): Shallow tectonics on the middle continental slope of the northeastern Gulf of Cadiz continental margin (SW Iberia). *Summaries of the VIII Symposium* MIA. Malaga (Spain). 149–152.

Manuscrito recibido el 28-10-2016
Recibida la revisión el 23-1-2017
Aceptado el manuscrito revisado el 24-1-2017